

Nonlinear transfer and spectral distribution of energy in α turbulence

Chuong V. Tran

*Department of Mathematical and Statistical Sciences, University of Alberta,
Edmonton, Alberta, Canada, T6G 2G1*

Abstract

Two-dimensional turbulence governed by the so-called α turbulence equations, which include the surface quasi-geostrophic equation ($\alpha = 1$), the Navier–Stokes system ($\alpha = 2$), and the governing equation for a shallow flow on a rotating domain driven by a uniform internal heating ($\alpha = 3$), is studied here in both the unbounded and doubly periodic domains. This family of equations conserves two inviscid invariants (energy and enstrophy in the Navier–Stokes case), the dynamics of which are believed to undergo a dual cascade. It is shown that an inverse cascade can exist in the absence of a direct cascade and that the latter is possible only when the inverse transfer rate of the inverse-cascading quantity approaches its own injection rate. Constraints on the spectral exponents in the wavenumber ranges lower and higher than the injection range are derived. For Navier–Stokes turbulence with moderate Reynolds numbers, the realization of an inverse energy cascade in the complete absence of a direct enstrophy cascade is confirmed by numerical simulations.

Key words:

α turbulence, Dual cascade, Energy spectra

PACS: 47.27.Ak, 47.52.+j, 47.27.Gs

1 Introduction

Incompressible fluid turbulence in two dimensions has always been a subject of interest because of its relative simplicity and broad applications in geophysical problems. Although the theory of two-dimensional (2D) turbulence is not strictly applicable to a geophysical fluid, the third (vertical) dimension

Email address: chuong@math.ualberta.ca (Chuong V. Tran).

in many geophysical systems can nevertheless be “removed”, and the resulting 2D equations are thought to be quantitatively adequate for describing the large-scale horizontal motion.

Some systems in this category, which receive considerable attention, are the surface quasi-geostrophic (SQG) equation, describing the motion of a rotating stratified fluid [3,15]; the “rotating shallow flow” (RSF) equation, governing the motion of a thin fluid on a rotating domain [35]; and the Charney–Hasegawa–Mima equation, governing the potential vorticity of an equivalent-barotropic fluid [6,13,14]. Except possibly for the last equation, these systems, together with the more familiar 2D Navier–Stokes (NS) equations, can be studied within a unified framework by a family of models (known as the α turbulence equations) indexed by a parameter $\alpha \in (0, \infty)$ [23]. Like the 2D NS system, the nonlinear transfer of α turbulence conserves two quadratic invariants: $\Psi_\alpha = \int_0^\infty \Psi_\alpha(k) dk$ and $\Psi_{2\alpha} = \int_0^\infty \Psi_{2\alpha}(k) dk$, where $\Psi_\theta(k) = k^\theta \Psi(k)$, $\Psi(k)$ is the streamfunction power spectrum, θ is a real number, and k is the wavenumber. Note that $\Psi_2(k)$ is the kinetic energy spectrum, and Ψ_2 is the kinetic energy.

The statistical dynamics of unbounded 2D NS turbulence are believed to achieve a quasi-steady state which simultaneously exhibits a direct enstrophy cascade to high wavenumbers and an inverse energy cascade to low wavenumbers. According to the classical theory formulated by Kraichnan [16,17], Leith [18], and Batchelor [2] (hereafter referred to as KLB), if the system is excited around a (forcing) wavenumber s , the dual cascade is supposed to carry virtually all of the energy input to ever-lower wavenumbers, down to wavenumber $k = 0$, and the enstrophy input to a high wavenumber $k_\nu \gg s$, around which the enstrophy is dissipated. Analyses based on Kolmogorov’s phenomenology predict that the energy spectrum scales respectively as $k^{-5/3}$ and k^{-3} in the energy- and enstrophy-cascading ranges (also known as inertial ranges). The KLB theory, when applied to α turbulence, implies the possibility that Ψ_α cascades to low wavenumbers and that $\Psi_{2\alpha}$ cascades to high wavenumbers. These (possible cascading) invariants correspond to different physical quantities for different flows. For SQG turbulence, the direct-cascading candidate is the energy. For RSF turbulence, the direct-cascading candidate is the palinstrophy. When $\alpha = 4$, the enstrophy becomes the inverse-cascading candidate. NS turbulence features the energy and enstrophy as the possible inverse- and direct-cascading quantities, respectively.

Despite numerical evidence confirming the realization of an inverse energy cascade and of the Kolmogorov–Kraichnan $k^{-5/3}$ spectrum [4,5,12,19,32], the dual cascade remains conjectural. No convincing evidence exists of a direct enstrophy cascade. Rather, there exist some negative results with respect to this problem. In particular, for a bounded system in equilibrium, a direct enstrophy cascade is excluded [33]. For an unbounded system, a direct enstrophy

cascade is prohibited for all weak inverse energy cascades [32]. By “weak”, it is understood that the inverse cascades do not carry virtually all of the energy input to the large scales. This behaviour is presumably the dynamical behaviour for finite-Reynolds number turbulence. The questions then arise whether the inverse energy cascade can become “strong” in the limit of infinite Reynolds number and whether a direct enstrophy cascade can then be realizable.

This study generalizes various previous results for the 2D NS system [30,32,33] to α turbulence and re-examines the dual-cascade hypothesis under the general framework of the latter case. Also, some new results on related issues, such as the non-conservative transfer of quadratic quantities other than the invariants, are reported. First, the derivations of some a priori estimates for the dissipation terms of the quadratic invariants are presented. Second, the result of Tran and Shepherd [33] is generalized to the present problem, showing that under the influence of a viscous operator, the invariants satisfy $\Psi_{2\alpha} \leq s^\alpha \Psi_\alpha$. Third, the conservative transfer of the quadratic invariants and the non-conservative transfer of other quadratic quantities are examined. The former consideration is essentially a reformulation of the dual-cascade hypothesis. It is shown that even in the limit of infinite Reynolds number, the inverse cascade of Ψ_α could become strong, carrying virtually all of the injection of Ψ_α to ever-larger scales, in the complete absence of a direct cascade of $\Psi_{2\alpha}$. This study does not attempt an alternative to the classical dual-cascade theory, but is concerned with the plausibility of the dual-cascade hypothesis. A constraint on the spectral slopes for fluids in equilibrium is obtained by extending the derivations of Tran and Bowman [30,32] to the present case. Finally, the results from numerical simulations of NS turbulence are presented, confirming the realization of an inverse energy cascade in the absence of a direct enstrophy cascade. These numerical results suggest that for high Reynolds numbers, the turbulence would become non-direct-cascading by evolving through a transient direct-cascading stage.

The remainder of this paper is organized as follows. Section 2 describes the equation of motion governing α turbulence and its conservation laws. Section 3 presents the derivations of the upper bounds on the asymptotic averages of the dissipation of quadratic invariants and the dynamical constraint $\Psi_{2\alpha} \leq s^\alpha \Psi_\alpha$. Section 4 reports an analysis concerning the plausibility of a direct cascade in unbounded fluids. Section 5 features a proof of the creation and depletion of quadratic quantities other than the invariants. Section 6 presents a constraint on the spectral slopes of the kinetic energy spectrum for fluids in equilibrium. Section 7 reports the results from numerical simulations of 2D NS turbulence, confirming the realization of a weak inverse energy cascade in the complete absence of a direct enstrophy cascade. The paper ends with some concluding remarks in the final section.

2 Governing equation

The term “ α turbulence” refers to a general class of 2D incompressible fluid turbulence, in which the conserved scalar $(-\Delta)^{\alpha/2}\psi$ is advected in a velocity field with stream function ψ . Here, α is a positive number, and Δ is the 2D Laplacian. The equation governing the fluid motion is

$$\partial_t(-\Delta)^{\alpha/2}\psi + J(\psi, (-\Delta)^{\alpha/2}\psi) = -\nu_\mu(-\Delta)^\mu(-\Delta)^{\alpha/2}\psi + f, \quad (1)$$

where $J(\varphi, \phi) = \partial_x\varphi\partial_y\phi - \partial_x\phi\partial_y\varphi$, $\nu_\mu > 0$ is the generalized viscosity coefficient, $\mu \geq 0$ is the degree of viscosity, and f is the forcing. The stream function $\psi(x, y, t)$ is related to the fluid velocity \mathbf{u} by $\mathbf{u} = (-\partial_y\psi, \partial_x\psi)$. This family includes the three physically realizable fluid systems, which are the focus of this work. The case $\alpha = 1$ corresponds to the SQG equation from the geophysical context, describing the motion of a stratified fluid with small Rossby and Ekman numbers [3,15,23]. The familiar 2D NS system corresponds to $\alpha = 2$. The case $\alpha = 3$ corresponds to the RSF system, governing a shallow flow on a rotating domain with uniform internal heating [35].

The nonlinear term in (1) obeys the conservation laws

$$\langle \psi J(\psi, (-\Delta)^{\alpha/2}\psi) \rangle = \langle (-\Delta)^{\alpha/2}\psi J(\psi, (-\Delta)^{\alpha/2}\psi) \rangle = 0, \quad (2)$$

where $\langle \cdot \rangle$ denotes the spatial average. As a consequence, the two quadratic quantities $\Psi_\alpha = \frac{1}{2}\langle |(-\Delta)^{\alpha/4}\psi|^2 \rangle$ and $\Psi_{2\alpha} = \frac{1}{2}\langle |(-\Delta)^{\alpha/2}\psi|^2 \rangle$ are conserved by nonlinear transfer.

In this study, f is assumed to be spectrally confined to a finite band of the wavenumber $K = [k_1, k_2]$, where $k_1 > 0$. More restrictive conditions on f and specific values of μ for the particular cases to be considered will be stated in due course. In particular, $\mu = 1$ represents molecular viscosity as in the NS case. The SQG system has $\mu = 1/2$ as the physical dissipation mechanism; other values of μ have also been considered for numerical purposes in the literature [21,25,26,28]. It is not well understood how the dynamics would depend on the degree of viscosity μ . Nevertheless, there appears to be a belief that $\nu_\mu(-\Delta)^\mu$ (for large positive values of μ) globally acts on the small scales, hence the name “small-scale dissipation”. This belief is associated with the concepts of direct cascade and of dissipation range and is incorrect if a direct cascade is not realizable. For example, for 2D NS turbulence in equilibrium, with $\nu_\mu(-\Delta)^\mu$ ($\mu > 0$) the only form of dissipation, the dissipation of energy (enstrophy) occurs mainly in the large scales (around the forcing scale) [33]. This example means that there exists no dissipation range well separated from the forcing scale and that the viscous operator $\nu_\mu(-\Delta)^\mu$ would have to be

correctly termed “large-scale dissipation”. In this case, the degree of viscosity μ plays an important role in the spectral distribution of energy [30,33].

The problem of nonlinear transfer and spectral distribution of quadratic quantities such as energy and enstrophy is best handled in wavenumber space. Hence, it is convenient to formulate the present problem accordingly. The power spectrum $\Psi_\theta(k)$, which represents the power density of $(-\Delta)^{\theta/4}\psi$ (for real θ) associated with the wavenumber k , is defined by

$$\Psi_\theta(k) = \frac{1}{2} \int_{|\boldsymbol{\ell}=k} |(-\Delta)^{\theta/4}\widehat{\psi}(\boldsymbol{\ell})|^2 d\boldsymbol{\ell} = \frac{1}{2} k^\theta \int_{|\boldsymbol{\ell}=k} |\widehat{\psi}(\boldsymbol{\ell})|^2 d\boldsymbol{\ell}, \quad (3)$$

where $\widehat{\psi}(\boldsymbol{\ell})$ is the Fourier transform of ψ , and the integral is over all wavevectors $\boldsymbol{\ell}$ having magnitude k . In this paper, most results apply to both unbounded and periodic (bounded) cases; the integral over continuous wavenumbers is then understood as the corresponding sum over discrete wavenumbers for the bounded case. The evolution of $\Psi_\alpha(k)$ is governed by

$$\frac{d}{dt}\Psi_\alpha(k) = T_\alpha(k) - 2\nu_\mu k^{2\mu}\Psi_\alpha(k) + F(k). \quad (4)$$

Here, $T_\alpha(k)$ and $F(k)$ are, respectively, the spectral transfer and input functions. (See [11,16] for the familiar NS case.) By virtue of the conservation laws (2), the transfer function $T_\alpha(k)$ satisfies

$$\int_0^\infty T_\alpha(k) dk = \int_0^\infty k^\alpha T_\alpha(k) dk = 0. \quad (5)$$

3 Asymptotic analysis

In this section, several a priori estimates of some relevant dynamical quantities are derived, and their implications for power-law scaling of the energy spectrum are discussed. The results obtained include upper bounds on the asymptotic averages of the dissipation of Ψ_α and $\Psi_{2\alpha}$ and an upper bound on $\Psi_{2\alpha}$ in terms of Ψ_α and the forcing wavenumber.

On multiplying (1) by ψ and $(-\Delta)^{\alpha/2}\psi$ and taking the spatial averages of the resulting equations, noting from the conservation laws that the nonlinear terms identically vanish, one obtains evolution equations for Ψ_α and $\Psi_{2\alpha}$,

$$\frac{d}{dt}\Psi_\alpha = -2\nu_\mu\Psi_{2\mu+\alpha} + \langle\psi f\rangle, \quad (6)$$

$$\frac{d}{dt}\Psi_{2\alpha} = -2\nu_\mu\Psi_{2\mu+2\alpha} + \langle(-\Delta)^{\alpha/2}\psi f\rangle. \quad (7)$$

Using the Cauchy–Schwarz and Young inequalities and because the forcing spectral support is confined to the wavenumber interval $[k_1, k_2]$, one obtains the upper bounds on the injection terms in (6) and (7):

$$\begin{aligned} \langle\psi f\rangle &\leq \langle|(-\Delta)^{\mu/2+\alpha/4}\psi|^2\rangle^{1/2}\langle|(-\Delta)^{-\mu/2-\alpha/4}f|^2\rangle^{1/2} \\ &\leq \nu_\mu\Psi_{2\mu+\alpha} + \frac{1}{2\nu_\mu}\langle|(-\Delta)^{-\mu/2-\alpha/4}f|^2\rangle \\ &\leq \nu_\mu\Psi_{2\mu+\alpha} + \frac{\langle|f|^2\rangle}{2\nu_\mu k_1^{2\mu+\alpha}}, \\ \langle(-\Delta)^{\alpha/2}\psi f\rangle &\leq \langle|(-\Delta)^{\mu/2+\alpha/2}\psi|^2\rangle^{1/2}\langle|(-\Delta)^{-\mu/2}f|^2\rangle^{1/2} \\ &\leq \nu_\mu\Psi_{2\mu+2\alpha} + \frac{1}{2\nu_\mu}\langle|(-\Delta)^{-\mu/2}f|^2\rangle \\ &\leq \nu_\mu\Psi_{2\mu+2\alpha} + \frac{\langle|f|^2\rangle}{2\nu_\mu k_1^{2\mu}}. \end{aligned} \quad (8)$$

The substitution of (8) in (6) and (7) yields

$$\begin{aligned} \frac{d}{dt}\Psi_\alpha &\leq -\nu_\mu\Psi_{2\mu+\alpha} + \frac{\langle|f|^2\rangle}{2\nu_\mu k_1^{2\mu+\alpha}}, \\ \frac{d}{dt}\Psi_{2\alpha} &\leq -\nu_\mu\Psi_{2\mu+2\alpha} + \frac{\langle|f|^2\rangle}{2\nu_\mu k_1^{2\mu}}. \end{aligned} \quad (9)$$

These inequalities readily admit the upper bounds on the asymptotic averages of $\Psi_{2\mu+\alpha}$ and $\Psi_{2\mu+2\alpha}$:

$$\limsup_{t\rightarrow\infty} \frac{1}{t} \int_0^t \Psi_{2\mu+\alpha} \, d\tau \leq \frac{1}{2\nu_\mu^2 k_1^{2\mu+\alpha}} \limsup_{t\rightarrow\infty} \frac{1}{t} \int_0^t \langle|f|^2\rangle \, d\tau, \quad (10)$$

$$\limsup_{t\rightarrow\infty} \frac{1}{t} \int_0^t \Psi_{2\mu+2\alpha} \, d\tau \leq \frac{1}{2\nu_\mu^2 k_1^{2\mu}} \limsup_{t\rightarrow\infty} \frac{1}{t} \int_0^t \langle|f|^2\rangle \, d\tau. \quad (11)$$

For a time-independent forcing f , the asymptotic average on the right-hand sides of (10) and (11) reduces to $\langle|f|^2\rangle$.

The upper bound (10) on the asymptotic average of $\Psi_{2\mu+\alpha}$ is interesting, particularly for the unbounded case. This bound prohibits the spectrum $\Psi_{2\mu+\alpha}(k)$ [$\Psi_\alpha(k)$] from acquiring a spectral scaling not shallower than k^{-1} [$k^{-2\mu-1}$] in

the limit $k \rightarrow 0$ because otherwise, a divergence of $\Psi_{2\mu+\alpha}$ would entail. This means that a constant inverse flux of Ψ_α (if it is realizable) ought to proceed toward $k = 0$ (in the limit $t \rightarrow \infty$) via a spectrum $\Psi_\alpha(k)$ shallower than $k^{-2\mu-1}$. This observation is intuitively obvious from the physical point of view: the proceeding of a sustainable inverse cascade is incompatible with a persistent increase in the dissipation of the inverse-cascading quantity. Note that the critical scaling $\Psi_\alpha(k) \propto k^{-2\mu-1}$ (for $k < k_1$) may be realizable only down to a finite wavenumber $k_0 > 0$ and necessarily corresponds to an asymptotic absolute equilibrium of Ψ_α .

For the NS system ($\alpha = 2$ and $\mu = 1$), $\Psi_{2\mu+\alpha} = \Psi_4$ (the enstrophy) is the dissipation agent of the energy Ψ_2 . The above analysis implies that the enstrophy (energy) spectrum in the inverse-cascading region is no steeper than k^{-1} (k^{-3}). This constraint turns out to be “generous”, as the Kolmogorov–Kraichnan $k^{-5/3}$ energy spectrum is much shallower than k^{-3} . For SQG turbulence ($\alpha = 1$ and $\mu = 1/2$), the energy Ψ_2 is the dissipation agent of the inverse-cascading candidate Ψ_1 . Hence, the energy asymptotic average is bounded. This condition requires that $\Psi_2(k)$ in the low-wavenumber region be no steeper than k^{-1} . Tran and Bowman [31] have previously noted this requirement.

Remark 1. Like the constraint in the NS case, the constraint on the spectral steepness of the low-wavenumber region for SQG turbulence is the threshold at which an inverse cascade is not sustainable. To allow for a steady positive growth rate of Ψ_1 , an energy spectrum shallower than k^{-1} in the low-wavenumber range is required.

A result derived by Tran and Shepherd [33] for NS turbulence confined to a doubly periodic domain is now generalized to the present problem. For simplicity, it is assumed that the forcing satisfies $s^\alpha \langle \psi f \rangle = \langle (-\Delta)^{\alpha/2} \psi f \rangle$, where s is some (constant) wavenumber. (The result to follow can be readily generalized to a less restrictive forcing class [33].) This condition can be realized in several ways. The simplest example [33] is the case of a monoscale forcing at a wavenumber s , i.e. a forcing f for which $(-\Delta)^\theta f = s^{2\theta} f$. Another example [27,30,32,33] is

$$\widehat{f}(\mathbf{k}) = \frac{\epsilon}{|K|} \frac{\widehat{\psi}(\mathbf{k})}{2\Psi(k)}, \quad (12)$$

for $k \in K = [k_1, k_2]$, and $\widehat{f}(\mathbf{k}) = 0$ otherwise. Here, ϵ is a positive number, and $|K|$ is the width (the number of discrete wavenumbers) of the forcing band for the continuous (discrete) case. For this forcing, the spectral injection rate of $\Psi_\alpha(k)$ is $F(k) = \epsilon/|K|$. Hence, the respective injection rates of Ψ_α and $\Psi_{2\alpha}$ are given by

$$\int_K F(k) dk = \epsilon, \quad (13)$$

$$\int_K k^\alpha F(k) dk = \frac{\epsilon}{|K|} \int_K k^\alpha dk = s^\alpha \epsilon, \quad (14)$$

where s^α is the mean of k^α over the forcing band K . This forcing is used in the numerical simulations of Section 7, where ϵ is a constant, yielding constant injection rates.

Multiplying (6) by s^α and subtracting the resulting equation from (7), noting that the forcing terms cancel, one obtains

$$\frac{d}{dt}(\Psi_{2\alpha} - s^\alpha \Psi_\alpha) = 2\nu_\mu (s^\alpha \Psi_{2\mu+\alpha} - \Psi_{2\mu+2\alpha}). \quad (15)$$

The difference on the right-hand side can be written as

$$s^\alpha \Psi_{2\mu+\alpha} - \Psi_{2\mu+2\alpha} = -s^{2\mu}(\Psi_{2\alpha} - s^\alpha \Psi_\alpha) - \int_0^\infty (s^{2\mu} - k^{2\mu})(s^\alpha - k^\alpha) \Psi_\alpha(k) dk.$$

Substituting this expression into (15) yields

$$\frac{d}{dt}(\Psi_{2\alpha} - s^\alpha \Psi_\alpha) = -2\nu_\mu s^{2\mu}(\Psi_{2\alpha} - s^\alpha \Psi_\alpha) - 2\nu_\mu \int_0^\infty (s^{2\mu} - k^{2\mu})(s^\alpha - k^\alpha) \Psi_\alpha(k) dk. \quad (16)$$

For $\mu \geq 0$ and $\alpha > 0$, the integral in (16) is non-negative. The first order equation (16) is dissipative and forced by a non-positive term. It follows that $\Psi_{2\alpha} - s^\alpha \Psi_\alpha$ becomes non-positive as $t \rightarrow \infty$. Hence, the constraint

$$\Psi_{2\alpha} \leq s^\alpha \Psi_\alpha \quad (17)$$

holds asymptotically.

Remark 2. Actually, the constraint (17) holds for all $t \geq T$, where T is a finite time determined by the initial condition, except for some trivial cases, which are rather irrelevant in the context of turbulence (see [33]). This constraint is mathematically interesting in the bounded case, as the inequality is in the opposite sense to Sobolev-type inequalities. In an unbounded domain where Ψ_α may grow unbounded whether or not an inverse cascade exists, (17) becomes obvious.

Remark 3. The dynamical constraint (17) holds if the single viscous operator is replaced by a combination $\sum_{\mu} \nu_{\mu} (-\Delta)^{\mu}$ for $\nu_{\mu}, \mu \geq 0$, where the summation is taken over all dissipation channels involved [33]. It also holds, with s replaced by k_2 , for a forcing satisfying $k_1^{\alpha} \int_K F(k) dk \leq \int_K k^{\alpha} F(k) dk \leq k_2^{\alpha} \int_K F(k) dk$. This double inequality automatically holds for any non-negative spectral injection, i.e. $F(k) \geq 0$ for all $k \in K$.

4 Conservative transfer

This section examines the nonlinear transfer of the quadratic invariants and their dynamical behaviours, particularly the possibility of a direct cascade of $\Psi_{2\alpha}$. A Fjørtoft-type analysis [10] concerning the collective transfer of all nonlinearly interacting triads is presented. The simple technique of Tran and Bowman [32] is employed in deriving a constraint on the spectral slope of the supposed direct-cascading range in terms of the growth rate of the inverse-cascading candidate and the dissipation wavenumber. These analyses finally lead to a self-consistent dynamical picture, which exhibits no direct cascade.

4.1 Inverse vs. direct transfer

Due to the conservation laws (5), the nonlinear transfer of Ψ_{α} and $\Psi_{2\alpha}$ obeys certain restrictions. Suppose that an initial Ψ_{α}^0 at wavenumber s , which corresponds to an initial $\Psi_{2\alpha}^0 = s^{\alpha} \Psi_{\alpha}^0$, is nonlinearly redistributed in wavenumber space. Because of the conservation of $\Psi_{2\alpha}$, the redistribution of an amount Ψ_{α}^+ beyond some given wavenumber $k_+ > s$ must satisfy $k_+^{\alpha} \Psi_{\alpha}^+ < s^{\alpha} \Psi_{\alpha}^0$, or equivalently, $\Psi_{\alpha}^+ / \Psi_{\alpha}^0 < (s/k_+)^{\alpha}$. Hence, no significant fractions of Ψ_{α}^0 are allowed to be transferred toward wavenumbers $k \gg s$. This condition corresponds to the well-known prohibition of a direct cascade of energy in the NS case. The constraint is more severe for a larger α in the sense that a larger α implies a smaller permissible Ψ_{α}^+ to be redistributed beyond a given $k_+ > s$. Similarly, due to the conservation of Ψ_{α} , the redistribution of an amount $s^{\alpha} \Psi_{\alpha}^-$ to the wavenumbers lower than some given wavenumber $k_- < s$ must satisfy $s^{\alpha} \Psi_{\alpha}^- / k_-^{\alpha} < \Psi_{\alpha}^0$, or equivalently, $s^{\alpha} \Psi_{\alpha}^- / (s^{\alpha} \Psi_{\alpha}^0) < (k_-/s)^{\alpha}$. Hence, no significant fractions of $s^{\alpha} \Psi_{\alpha}^0$ are allowed to be transferred toward wavenumbers $k \ll s$. On the other hand, the redistribution of any amount $\Psi'_{\alpha} < \Psi_{\alpha}^0$ toward the vanishing wavenumbers is permitted. Such a transfer induces a loss of $s^{\alpha} \Psi'_{\alpha}$ in $\Psi_{2\alpha}$. The conservation of $\Psi_{2\alpha}$ then requires that the remainder $\Psi_{\alpha}^0 - \Psi'_{\alpha}$ be redistributed toward the high wavenumbers, to make up for the lost amount $s^{\alpha} \Psi'_{\alpha}$. For a non-negligible remainder $\Psi_{\alpha}^0 - \Psi'_{\alpha}$ and large α , the lost amount $s^{\alpha} \Psi'_{\alpha}$ can be recovered with a redistribution of $\Psi_{\alpha}^0 - \Psi'_{\alpha}$ toward wavenumbers slightly larger than s , resulting in no direct cascade. This means

that a direct cascade is possible only in the limit $\Psi'_\alpha \rightarrow \Psi_\alpha^0$. In other words, an inverse cascade can exist in the complete absence of a direct cascade, and the latter is not permitted until virtually all of Ψ_α cascades to the vanishing wavenumbers. This observation is consistent with the results from numerical simulations of 2D NS turbulence that have found an inverse energy cascade, regardless of what happened to the enstrophy [4,5,12,32].

4.2 Constraint on spectral slope for $k > s$

A more quantitative version of the preceding analysis is in order. The dual-cascade scenario is now examined in the framework of the forced-dissipative picture. A constraint on the spectral slope of the supposed direct-cascading range is derived in terms of the growth rate of Ψ_α and the dissipation wavenumber.

The evolution of Ψ_α and $\Psi_{2\alpha}$ is governed by

$$\frac{d}{dt}\Psi_\alpha = -2\nu_\mu\Psi_{2\mu+\alpha} + \int_K F(k) dk, \quad (18)$$

$$\frac{d}{dt}\Psi_{2\alpha} = -2\nu_\mu\Psi_{2\mu+2\alpha} + \int_K k^\alpha F(k) dk. \quad (19)$$

Let us consider quasi-steady dynamics, where a steady spectrum has been established down to a wavenumber $k_0 \ll s$. The injections have become steady and satisfy $s^\alpha \int_K F(k) dk = \int_K k^\alpha F(k) dk$, where s is a wavenumber in the forcing region. The evolution of $\Psi_{2\alpha}$ has reached equilibrium, while Ψ_α continues to cascade toward wavenumbers $k < k_0$ at a steady growth rate $d\Psi_\alpha/dt = \epsilon_0$.¹ It follows from (18) and (19) that

$$\frac{\Psi_{2\mu+2\alpha}}{\Psi_{2\mu+\alpha}} = s^\alpha \frac{\epsilon}{\epsilon - \epsilon_0}, \quad (20)$$

where $\epsilon = \int_K F(k) dk$. For simplicity, it is assumed that the quasi-steady spectrum $\Psi_\alpha(k)$ can be approximated by [30]

$$\Psi_\alpha(k) = \begin{cases} ak^{-\gamma} & \text{if } k_0 < k < s, \\ bk^{-\beta} & \text{if } s < k < k_\nu, \end{cases} \quad (21)$$

¹ It should be emphasized that although evidence exists of an inverse cascade for various values of α , one cannot be sure that an inverse cascade exists for all $\alpha > 0$. Section 6 deals with the non-cascading case $\epsilon_0 = 0$, which is applicable to both bounded and unbounded systems in equilibrium.

where a , b , γ , β are constants, and k_ν is the highest wavenumber in the range $k^{-\beta}$, beyond which the spectrum is supposed to be steeper than $k^{-\beta}$. The ratio on the left-hand side of (20) can be estimated as

$$\begin{aligned} \frac{\Psi_{2\mu+2\alpha}}{\Psi_{2\mu+\alpha}} &\geq \frac{a \int_{k_0}^s k^{2\mu+\alpha-\gamma} dk + b \int_s^{k_\nu} k^{2\mu+\alpha-\beta} dk}{a \int_{k_0}^s k^{2\mu-\gamma} dk + b \int_s^\infty k^{2\mu-\beta} dk} \\ &= s^\alpha \frac{\int_{k_0/s}^1 \kappa^{2\mu+\alpha-\gamma} d\kappa + \int_{s/k_\nu}^1 \kappa^{\beta-2\mu-\alpha} d\kappa}{\int_{k_0/s}^1 \kappa^{2\mu-\gamma} d\kappa + \int_0^1 \kappa^{\beta-2\mu} d\kappa}. \end{aligned} \quad (22)$$

The inequality results from dropping from the estimate of $\Psi_{2\mu+2\alpha}$ the spectral contribution beyond k_ν and extending the range $bk^{-\beta}$ to infinity in the estimate of $\Psi_{2\mu+\alpha}$. The equality is obtained by making the respective substitutions $\kappa = k/s$ and $\kappa = s/k$ in the two integrals in each of the numerator and denominator plus the continuity relation $as^{-\gamma} = bs^{-\beta}$. It follows that

$$\frac{\int_{s/k_\nu}^1 \kappa^{\beta-2\mu-\alpha-2} d\kappa}{\int_{k_0/s}^1 \kappa^{2\mu-\gamma} d\kappa + \int_0^1 \kappa^{\beta-2\mu-2} d\kappa} \leq \frac{\epsilon}{\epsilon - \epsilon_0}. \quad (23)$$

A direct cascade of $\Psi_{2\alpha}$ requires that its dissipation occurs primarily in the small scales. Accordingly, the spectrum $\Psi_{2\mu+2\alpha}(k)$ must be shallower than k^{-1} . It is interesting to consider the regime where the onset of direct-cascading dynamics is possible, i.e., the regime for which $\Psi_{2\mu+2\alpha}(k)$ approximately scales as k^{-1} for $k > s$. This scaling means $-\beta + 2\mu + \alpha \approx -1$, or equivalently $\beta - 2\mu - 2 \approx \alpha - 1$. The second integral in the denominator on the left-hand side of (23) is then of order unity (or smaller if $\alpha \gg 1$). Now it is seen in Section 3 that a persistent inverse cascade ($\epsilon_0 > 0$) requires that $\Psi_{2\mu+\alpha}(k)$ be shallower than k^{-1} in the inverse-cascading range, i.e. $2\mu - \gamma > -1$. This requirement implies that the first integral in the denominator on the left-hand side of (23) is of order unity. Hence, the denominator on the left-hand side of (23) is of order unity. On the other hand, the integral in the numerator can be significantly larger than unity. In particular, this integral approaches the value $\ln(k_\nu/s)$ in the limit $\beta - 2\mu - \alpha - 1 \rightarrow 0$ and can be large for a large ratio k_ν/s . This result implies that the left-hand side of (23) can be significantly larger than unity in the non-direct-cascading regime. The constraint (23) then requires that ϵ_0 be sufficiently close to ϵ . Hence, an inverse cascade with various strength (various values of the ratio ϵ_0/ϵ) can exist in the absence of a direct cascade, as was previously argued in this section without an explicit dissipation mechanism. Finally, in the limit $s/k_\nu \rightarrow 0$, as is commonly assumed for high-Reynolds number turbulence, a direct cascade, regardless of the spectral slope $-\beta$, requires the limit $\epsilon_0 \rightarrow \epsilon$.

Remark 4. For NS turbulence, the critical slope of the energy spectrum,

for $k > s$, at the onset of a possible direct cascade is -5 . The KLB direct-
 enstrophy-cascading range scales as k^{-3} , which is much shallower than the
 critical scaling k^{-5} . (The spectral discrepancy between these two scaling laws
 is huge.) β has been proposed to have some favourable values between 3 and 5,
 according to the theories of Moffatt [20] ($\beta = 11/3$), Saffman [24] ($\beta = 4$), and
 Sulem and Frisch [29] ($\beta \leq 11/3$). For SQG turbulence, the critical slope is
 -2 . The Kolmogorov–Kraichnan direct-energy-cascading range scales as $k^{-5/3}$,
 which is slightly shallower than the critical scaling k^{-2} .

The question remains as to whether a direct cascade is realizable in unbounded
 fluids. The present analysis narrows down the possibility of a direct cascade
 to the regime in which the growth rate of Ψ_α approaches its own injection
 rate. If a direct cascade could be realizable and if a spectrum much shallower
 than the critical spectrum could be achieved (e.g., a k^{-3} scaling in NS turbu-
 lence), the critical scaling would intuitively be realizable at relatively moderate
 Reynolds numbers, and the direct-cascading range would become shallower as
 the Reynolds number increases. Numerical simulations may be able to probe
 into this critical regime and help assess the existence or non-existence of a
 direct cascade. Given the low resolutions available in current computers, a
 plausible possibility is to explore how ϵ_0 , β , and k_ν adjust with respect to the
 Reynolds number in the non-direct-cascading regime [32]. This information
 may then be extrapolated to the critical limit. A difficulty with this scheme
 is that one might not be able to get sufficiently close to the critical regime to
 make the extrapolation meaningful.²

4.3 A non-direct-cascading dynamical picture

It is interesting to consider a self-consistent dynamical picture, which is in
 accord with the preceding analysis and exhibits no direct cascade, even in
 the limit of infinite Reynolds number. This discussion is concerned with the
 plausibility of a direct cascade rather than with an attempt to find an alter-
 native to the dual-cascade theory. In the limit $\nu_\mu \rightarrow 0$, the equilibrium of
 $\Psi_{2\alpha}$ implies that $\Psi_{2\mu+2\alpha}$ diverges as ν_μ^{-1} . In the absence of a direct cascade,
 this condition can be accounted for by both the logarithmic divergence of
 $\ln(k_\nu/s)$, as $k_\nu \rightarrow \infty$, and an increase of b . The latter factor is relevant since
 it is not expected that k_ν grows exponentially as $\nu_\mu \rightarrow 0$. In any case, one has
 $s^\alpha \epsilon / 2\nu_\mu = \Psi_{2\mu+2\alpha} \geq b \ln(k_\nu/s)$. Meanwhile, $\Psi_{2\mu+\alpha}$ is given by

² For 2D NS turbulence, one would need several wavenumber decades to simulate
 an inverse energy cascade that carries about 90% of the injected energy to the large
 scales [32]. [This requirement can be readily deduced from (25).] This resolution is
 already a challenge for current computers. In fact, no numerical simulations per-
 formed thus far have achieved a resolution better than four wavenumber decades.

$$\Psi_{2\mu+\alpha} = bs^{-\alpha} \left(\frac{1}{2\mu+1-\gamma} + \frac{1}{\alpha} \right), \quad (24)$$

for $2\mu+1-\gamma > 0$. The dissipation of Ψ_α can be bounded from above by

$$2\nu_\mu \Psi_{2\mu+\alpha} \leq \frac{\epsilon}{\ln(k_\nu/s)} \left(\frac{1}{2\mu+1-\gamma} + \frac{1}{\alpha} \right). \quad (25)$$

This result implies that $2\nu_\mu \Psi_{2\mu+\alpha} \rightarrow 0$ as $k_\nu \rightarrow \infty$ ($\nu_\mu \rightarrow 0$). Hence, in the limit $\nu_\mu \rightarrow 0$, no direct cascade would be needed in order for an inverse cascade to proceed toward $k=0$, carrying with it virtually all of the input of Ψ_α . Thus, this hypothetical picture depicts non-direct-cascading dynamics for all Reynolds numbers. As ν_μ becomes ever smaller, the range $bk^{-\beta}$ gets ever wider, β gets ever closer to the critical value $\beta = 2\mu + \alpha + 1$, and b increases somewhat less rapidly than ν_μ^{-1} . Eventually, Ψ_θ (for all real θ) diverges as $\nu_\mu \rightarrow 0$. This feature is completely absent from the dual-cascade picture,³ where $\Psi_{2\mu+\alpha}$ is supposed to remain finite in the limit $\nu_\mu \rightarrow 0$. Note that the present discussion would apply to both bounded and unbounded systems. The only essential difference between these systems would be that for the bounded system, the inverse cascade is halted at the largest available scale, upon which significant departures in the dynamics of the two systems take place. The approach to equilibrium after the arrest of the inverse cascade in 2D NS turbulence was numerically studied by Borue [5]. Also, a physical interpretation of the observed k^{-3} spectrum at the large scales was given. Tran and Bowman [30,32] observed and explained a similar result.

The existence of a weak inverse energy cascade in the complete absence of a direct enstrophy cascade for moderate-Reynolds number NS turbulence is strongly supported by the theoretical arguments and numerical results of Tran and Bowman [30,32] and by the numerous numerical investigations targeted at the inverse cascade in the literature.⁴ Section 7 provides further numerical evidence for the realizability of non-direct-cascading dynamics. The results reported there also show the formation of an enstrophy range shallower than k^{-5} during the transient dynamics, thereby suggesting that the turbulence

³ In the dual-cascade picture, b is essentially insensitive to ν_μ in the limit $\nu_\mu \rightarrow 0$. The divergence of $\Psi_{2\mu+2\alpha}$, as $\nu_\mu \rightarrow 0$, is mainly due to the increase of k_ν . $\Psi_{2\mu+\alpha}$ (and possibly other quadratic quantities) remains finite in the limit $\nu_\mu \rightarrow 0$. Therefore, the dual-cascade picture poses a “sudden” blow-up at $\nu_\mu = 0$. This behaviour is somewhat harder to perceive than the “smooth” blow-up in the non-direct-cascading picture.

⁴ Those investigations inadvertently do not recognize the absence of a direct cascade for obvious reason: the forcing region is usually chosen as close as possible to the largest available wavenumber to obtain a wide inverse-cascading range, thereby allowing for no simultaneous observations of the enstrophy dynamics.

would become non-direct-cascading by evolving through a direct-cascading stage.

5 Non-conservative transfer

The creation and depletion of quadratic quantities other than the two invariants by nonlinear transfer are now investigated. For an arbitrary spectrum, subject to the finiteness of the quadratic quantities under consideration, one has the following interpolation-type inequality, which can be shown by Hölder's inequality:

$$\Psi_{\theta_2+\theta_3}^{\theta_1} \leq \Psi_{\theta_1+\theta_3}^{\theta_2} \Psi_{\theta_3}^{\theta_1-\theta_2}, \quad (26)$$

for $\theta_1 > \theta_2 > 0$ and θ_3 is an arbitrary real number. This inequality is geometry-independent, so that it applies to both bounded and unbounded cases. The equality occurs if and only if $\Psi(k) \neq 0$ is monoscale, i.e., if $\Psi(k)$ is nonzero only at a single wavenumber (a delta function for the case of continuous spectrum). This trivial case is excluded so that only the strict version of (26) is applied in what is to follow. By applying (26) with $(\theta_1, \theta_2, \theta_3) = (\alpha, \theta - \alpha, \alpha)$ one obtains

$$\Psi_\theta < \Psi_{2\alpha}^{\theta/\alpha-1} \Psi_\alpha^{2-\theta/\alpha} \quad \text{for } \theta \in (\alpha, 2\alpha). \quad (27)$$

Similarly, the two substitutions $(\theta_1, \theta_2, \theta_3) = (\theta - \alpha, \alpha, \alpha)$ and $(\theta_1, \theta_2, \theta_3) = (2\alpha - \theta, \alpha - \theta, \theta)$ into (26) yield

$$\Psi_\theta > \Psi_{2\alpha}^{\theta/\alpha-1} \Psi_\alpha^{2-\theta/\alpha} \quad \text{for } \theta \notin [\alpha, 2\alpha]. \quad (28)$$

The quantities on the right-hand sides of (27) and (28) are conserved by nonlinear transfer (because Ψ_α and $\Psi_{2\alpha}$ are invariant) and equal to Ψ_θ^0 , for an initial monoscale Ψ_θ^0 . Therefore, the subsequent nonlinear transfer necessarily results in the depletion (creation) of Ψ_θ for $\theta \in (\alpha, 2\alpha)$ ($\theta \notin [\alpha, 2\alpha]$). It should be noted that continuous increase (decrease) of the non-conserved quadratic quantities from an initial monoscale spectrum is possible but cannot be assured, due to the reversible nature of the inviscid problem.

The above picture, when applied to forced-dissipative systems in equilibrium or in quasi-steady dynamics, implies that the nonlinear transfer destroys (enhances) the injection of Ψ_θ from a monoscale forcing for $\theta \in (\alpha, 2\alpha)$ ($\theta \notin [\alpha, 2\alpha]$). In other words, the integrated transfer $\int_0^\infty k^{\theta-\alpha} T_\alpha(k) dk$ in the evolution equation

$$\frac{d}{dt}\Psi_\theta = \int_0^\infty k^{\theta-\alpha} T_\alpha(k) dk - 2\mu\Psi_{2\mu+\theta} + \int_K k^{\theta-\alpha} F(k) dk \quad (29)$$

is negative (positive) for $\theta \in (\alpha, 2\alpha)$ ($\theta \notin [\alpha, 2\alpha]$). To see this result explicitly, note that in equilibrium or quasi-steady dynamics, $T_\alpha(k) \geq 0$ for $k \neq s$ because $F(k) = 0$ for $k \neq s$, and the dissipation is non-negative [cf. (4)]. Similar to (26), the non-negative (and non-monoscale) transfer function $T_\alpha(k)$, for $k \neq s$, satisfies

$$\left(\int_{k \neq s} k^{\theta_2+\theta_3} T_\alpha(k) dk \right)^{\theta_1} < \left(\int_{k \neq s} k^{\theta_1+\theta_3} T_\alpha(k) dk \right)^{\theta_2} \left(\int_{k \neq s} k^{\theta_3} T_\alpha(k) dk \right)^{\theta_1-\theta_2} \quad (30)$$

for $\theta_1 > \theta_2 > 0$ and θ_3 is an arbitrary real number. Upon substituting $(\theta_1, \theta_2, \theta_3) = (\alpha, \theta - \alpha, 0)$ into (30) and using the conservation laws (5), one finds

$$\begin{aligned} \int_{k \neq s} k^{\theta-\alpha} T_\alpha(k) dk &< \left(\int_{k \neq s} k^\alpha T_\alpha(k) dk \right)^{\theta/\alpha-1} \left(\int_{k \neq s} T_\alpha(k) dk \right)^{2-\theta/\alpha} \\ &= (s^\alpha |T_\alpha(s)|)^{\theta/\alpha-1} |T_\alpha(s)|^{2-\theta/\alpha} = s^{\theta-\alpha} |T_\alpha(s)| \end{aligned} \quad (31)$$

for $\theta \in (\alpha, 2\alpha)$, or equivalently,

$$\int_0^\infty k^{\theta-\alpha} T_\alpha(k) dk < 0. \quad (32)$$

This result means that for $\theta \in (\alpha, 2\alpha)$, Ψ_θ is destroyed by nonlinear transfer. Similarly, with the substitutions $(\theta_1, \theta_2, \theta_3) = (\theta - \alpha, \alpha, 0)$ and $(\theta_1, \theta_2, \theta_3) = (2\alpha - \theta, \alpha - \theta, \theta - \alpha)$, one obtains

$$\int_0^\infty k^{\theta-\alpha} T_\alpha(k) dk > 0, \quad (33)$$

for $\theta \notin [\alpha, 2\alpha]$. This result means that for $\theta \notin [\alpha, 2\alpha]$, Ψ_θ is created by nonlinear transfer.

The creation and depletion of Ψ_θ for different values of α are interesting; here, only some typical cases are considered. For $\alpha < 2$, the enstrophy Ψ_4 (and vorticity) can be created. This enstrophy creation arguably occurs in SQG turbulence ($\alpha = 1$), as its inviscid unforced dynamics is known to resemble that of the three-dimensional Euler equation in many aspects, particularly

in the possibility of spontaneous development of singularities [7,9]. Note that the enstrophy creation need not be a consequence of a direct cascade and that the created enstrophy is subject to viscous dissipation in dissipative systems. For $2 < \alpha < 4$ such as in RSF turbulence ($\alpha = 3$), the energy is created while the enstrophy is destroyed. The creation of energy occurs toward the low wavenumbers and evades viscous dissipation. If an inverse cascade of Ψ_α proceeds toward $k = 0$ at a steady growth rate, the energy growth rate increases without bound. When $\alpha > 4$, both the energy and enstrophy are created, and this creation occurs toward the low wavenumbers. Both the energy and enstrophy growth rates increase without bound in the presence of a steady growth rate of Ψ_α . When $\alpha < 1$, both the energy and enstrophy are created, and this creation occurs toward the high wavenumbers. The NS system happens to have the critical value $\alpha = 2$, for which both the energy and enstrophy are conserved by advective nonlinearities.

6 Constraints on the slopes of equilibrium spectrum

For fluids in equilibrium, $\epsilon_0 = 0$ and (20) reduces to the balance equation $s^\alpha \Psi_{2\mu+\alpha} = \Psi_{2\mu+2\alpha}$. Assuming the spectral scaling (21) and following the calculations leading to (23), one obtains the estimate of $\Psi_{2\mu+2\alpha} - s^\alpha \Psi_{2\mu+\alpha}$:

$$\begin{aligned}
\int_{k_0}^{\infty} (k^\alpha - s^\alpha) k^{2\mu} \Psi_\alpha(k) dk &\geq a \int_{k_0}^s (k^\alpha - s^\alpha) k^{2\mu-\gamma} dk + b \int_s^{k_\nu} (k^\alpha - s^\alpha) k^{2\mu-\beta} dk \\
&= a s^{2\mu+\alpha+1-\gamma} \int_{k_0/s}^1 (\kappa^\alpha - 1) \kappa^{2\mu-\gamma} d\kappa \\
&\quad + b s^{2\mu+\alpha+1-\beta} \int_{s/k_\nu}^1 (1 - \kappa^\alpha) \kappa^{\beta-2\mu-\alpha-2} d\kappa \\
&= a s^{2\mu+\alpha+1-\gamma} \left(- \int_{k_0/s}^1 (1 - \kappa^\alpha) \kappa^{2\mu-\gamma} d\kappa + \int_{s/k_\nu}^1 (1 - \kappa^\alpha) \kappa^{\beta-2\mu-\alpha-2} d\kappa \right),
\end{aligned} \tag{34}$$

where the inequality results from dropping the spectral contribution beyond k_ν , the second line is obtained by the respective changes of variables $\kappa = k/s$ and $\kappa = s/k$ in the two integrals on the right-hand-side of the first line, and the third line is obtained by using the continuity relation $as^{-\gamma} = bs^{-\beta}$. Here, k_0 is the lowest wavenumber in the bounded case or a cutoff wavenumber in the unbounded case. Since the left-hand side of (34) vanishes, it can be deduced that

$$\int_{k_0/s}^1 (1 - \kappa^\alpha) \kappa^{2\mu - \gamma} d\kappa \geq \int_{s/k_\nu}^1 (1 - \kappa^\alpha) \kappa^{\beta - 2\mu - \alpha - 2} d\kappa. \quad (35)$$

For bounded high-Reynolds number turbulence driven at a relatively low wavenumber s , it is reasonable to assume that $k_0/s \geq s/k_\nu$. This condition requires $2\mu - \gamma \leq \beta - 2\mu - \alpha - 2$, as the integrals in (35) decrease if the corresponding powers of κ ($2\mu - \gamma$ and $\beta - 2\mu - \alpha - 2$) increase. It follows that $\gamma + \beta \geq 4\mu + \alpha + 2$.

On the other hand, the convergence of the right-hand integral in (35), as $s/k_\nu \rightarrow 0$, requires $\beta > 2\mu + \alpha + 1$. (Equivalently, $\Psi_{2\mu+2\alpha}(k)$ is steeper than k^{-1} for $k > s$.) That is, no direct cascade exists for equilibrium dynamics. The spectral contribution beyond k_ν which is dropped from (34) is then negligible and (35) is essentially an equality. It follows that $\gamma + \beta \approx 4\mu + \alpha + 2$ if $k_0/s \approx s/k_\nu$, and $\gamma + \beta$ can fall slightly below $4\mu + \alpha + 2$ if $k_0/s < s/k_\nu$. For both these cases, $\gamma \leq 2\mu + 1$, so that an inverse cascade is also ruled out because the dissipation of Ψ_α cannot occur at the largest scales. Although an inverse cascade cannot be ruled out in the case $k_0/s > s/k_\nu$, such a cascade, if realizable, would only be marginal and characteristically different from its unbounded counterpart in the classical picture.

It is more informative to write the constraint $\gamma + \beta \geq 4\mu + \alpha + 2$, for $k_0/s \geq s/k_\nu$, in terms of the slopes of the kinetic energy spectrum $\Psi_2(k)$. Let $-\tilde{\gamma}$ and $-\tilde{\beta}$ denote, respectively, the slopes of $\Psi_2(k)$ in the ranges of wavenumbers lower and higher than the forcing wavenumber; $\tilde{\gamma}$ and $\tilde{\beta}$ are then related to γ and β by $\tilde{\gamma} = \gamma + \alpha - 2$ and $\tilde{\beta} = \beta + \alpha - 2$. It follows that

$$\tilde{\gamma} + \tilde{\beta} \geq 4\mu + 3\alpha - 2. \quad (36)$$

This inequality reduces to $\tilde{\gamma} + \tilde{\beta} \geq 8$ for NS turbulence, $\tilde{\gamma} + \tilde{\beta} \geq 3$ for SQG turbulence, and $\tilde{\gamma} + \tilde{\beta} \geq 4\mu + 7$ for RSF turbulence.

Constantin [8] has studied the spectral scaling of SQG turbulence and derived the pointwise estimate $\Psi_2(k) \leq ck^{-2}$ in the wavenumber range $k < s$. Smith et al. [28] numerically explored this problem and found energy spectra considerably shallower than k^{-1} in this range. The “energy” spectrum plotted by Smith et al. [28] is $\Psi_1(k)$, and this spectrum appears to have a slope ≈ -1.5 . Hence, $\Psi_2(k)$ approximately scales⁵ as $k^{-0.5}$. Dimensional analyses predict the scaling $\Psi_2(k) \propto k^{-1}$ for $k < s$ [23,28]. The present estimate agrees with Smith

⁵ Note that Smith et al. [28] used linear drag in their simulations. Hence, the observed $k^{-0.5}$ scaling may in principle differ from that of SQG turbulence with the dissipation operator $(-\Delta)^{1/2}$. Nevertheless, their results provide strong evidence that the energy spectrum in the wavenumber range $k < s$ is shallower than k^{-1} .

et al.’s numerical results and with the prediction based on dimensional analyses better than with Constantin’s estimate. On physical grounds, a spectrum shallower than k^{-1} is more plausible, for two reasons. First, the prohibition of a significant inverse energy transfer in SQG turbulence (in marked contrast to the inverse energy cascade in NS turbulence) should render the energy spectrum in the wavenumber range $k < s$ shallower than k^{-1} because any spectra not shallower than k^{-1} would require a significant inverse energy transfer. Second, the hypoviscous dissipation of SQG dynamics, $(-\Delta)^{1/2}$, does not accommodate any energy spectra not shallower than k^{-1} in the low-wavenumber range (see Section 3).

In a recent laboratory experiment on a rapidly rotating fluid, Baroud et al. [1] observed a k^{-2} spectrum extending for almost two wavenumber decades lower than the forcing wavenumber. This result is consistent with the constraint $\tilde{\gamma} + \tilde{\beta} \geq 8$ obtained for the NS case, but cannot be explained within the context of SQG turbulence, for the reasons discussed above. A possible explanation for Baroud et al.’s result is that a rotating fluid, believed to be governed by the SQG equation,⁶ may still behave (to some extent) as a 2D NS fluid. Therefore, the dynamics of such a fluid might exhibit mixed characteristics of both SQG and NS turbulence. While a systematic analysis is required for a proper understanding of Baroud et al.’s experimental result, this hypothesis offers a possible explanation for the observed spectrum.

7 Numerical results

This section presents results from numerical simulations that confirm the realization of an inverse energy cascade in 2D NS turbulence, where energy is transferred to the large scales via the Kolmogorov–Kraichnan spectrum $k^{-5/3}$, in the absence of a direct cascade. These results provide numerical evidence (also see [32]) for the prediction and motivation for the discussion in the preceding sections. For the two sufficiently resolved Reynolds numbers, the energy growth rate ϵ_0 , calculated as the inverse cascade reaches $k \approx 3$, is larger for the higher Reynolds number. However, this preliminary attempt is in no position to address what happens in the high-Reynolds number regime.

Eq. (1) with $\alpha = 2$ and $\mu = 1$ is simulated in a doubly periodic square of side

⁶ The derivation of the SQG equation involves the temperature field [22,34]. More accurately, in order to arrive at the SQG equation, the vertical gradient of the temperature at the surface of a rotating stratified fluid is considered. Such a gradient is absent in Baroud et al.’s experiment since the fluid temperature is presumably constant throughout the rotating tank. Hence, the results in [1] cannot be attributed with certainty to SQG turbulence.

2π . The forcing $\widehat{f}(\mathbf{k})$ is given by (12), where $\epsilon = 1$ and $K = [49.5, 50.5]$. The enstrophy injection rate is $s^2\epsilon \approx 2500$, where $s^2 \approx 2500$ is the mean of k^2 over K . The attractive aspect of (12) is that it is steady, so that the uncertainty in the energy transfer rate ϵ_0 , which is calculated according to $\epsilon_0 = \epsilon - 2\nu_1\Psi_4$, is due solely to that of the enstrophy Ψ_4 . It is necessary to have a sufficiently wide inverse-cascading range, so that the enstrophy approaches its equilibrium value before finite-size effects interfere with the inverse cascade. It is also desirable to have a wide wavenumber range $k > s$, so that high Reynolds numbers can be achieved. For a given resolution, the choice of K is a compromise between these two considerations. With the present choice of K , the enstrophy calculated for a $k^{-5/3}$ spectrum in the wavenumber interval $[3, 50]$ is approximately 2% less than that calculated for the same spectrum in the interval $[0, 50]$. Hence, the energy transfer rate, which is calculated when the energy peak reaches wavenumber $k \approx 3$, may be greater than its projected value by a few percents (assuming no significant finite-size interference to the inverse cascade up to that point in time). Dealiased pseudospectral method is used with 1024^2 and 2048^2 total modes. Several different Reynolds numbers, corresponding to several different values of ν_1 , were simulated. The lower resolution was used for $\nu_1 = 7 \times 10^{-4}$; 5×10^{-4} , and the higher resolution was used for $\nu_1 = 3.5 \times 10^{-4}$; 2.5×10^{-4} ; 1.25×10^{-4} ; 6.25×10^{-5} . For all simulations, the initial energy spectrum had a negligibly small peak at the forcing wavenumber ($\Psi_2(50) \approx 10^{-10}$).

For $\nu_1 = 7 \times 10^{-4}$, the energy peak was observed to reach $k \approx 3$ at $t \approx 10.2$, upon which both the energy spectrum (see Fig. 1) and the total enstrophy were calculated (both time-averaged between $t = 10.2$ and $t = 10.3$). For a sense of this time scale, the dissipation time at the forcing wavenumber $s \approx 50$ is $t_s = (2\nu_1 s^2)^{-1} \approx 0.3$. The calculated value of enstrophy $\Psi_4 = 588$ amounts to an energy dissipation rate $2\nu_1\Psi_4 = 0.823$, accounting for 82% of the energy injection rate $\epsilon = 1$. The energy growth rate ϵ_0 is then 18% of the energy injection rate, due to the inverse energy cascade. It is evident from Fig. 1 that an inverse cascade is realizable in the complete absence of a direct cascade: the enstrophy range scales as $k^{-5.7}$, so that virtually all of the enstrophy is dissipated in the vicinity of the forcing region. For $\nu_1 = 5 \times 10^{-4}$, the energy peak was observed to reach $k \approx 3$ at $t \approx 8.8$, upon which both the energy spectrum (see Fig. 2) and the total enstrophy were calculated (both time-averaged between $t = 8.8$ and $t = 8.9$). The calculated value of enstrophy $\Psi_4 = 761$ amounts to an energy dissipation rate $2\nu_1\Psi_4 = 0.761$, accounting for 76% of the energy injection rate $\epsilon = 1$. The energy growth rate ϵ_0 is then 24% of the energy injection rate, due to the inverse energy cascade. The enstrophy range scales as $k^{-5.5}$, which is slightly shallower than its counterpart in the previous case. These results imply that the inverse cascade and the enstrophy-range spectrum get stronger and shallower, respectively, as the viscosity coefficient ν_1 decreases (the Reynolds number increases). Finally, for both cases, the inverse cascade carries only a small fraction of the energy input to the largest

scale and yet a $k^{-5/3}$ spectrum manifests itself nonetheless. This suggests that a $k^{-5/3}$ inverse-cascading range does not require the transfer of virtually all energy input to the large scales.

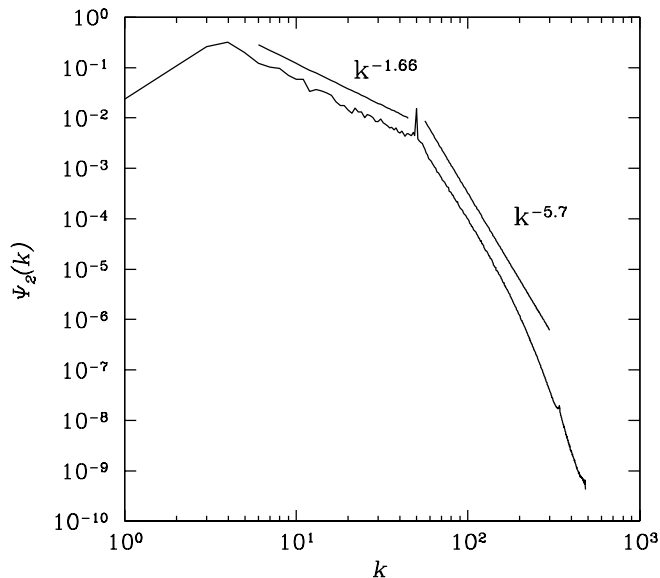


Fig. 1. The energy spectrum $\Psi_2(k)$ vs. k averaged between $t = 10.2$ and $t = 10.3$. The enstrophy averaged in the same period is $\Psi_4 = 588$. The energy injection rate and viscosity coefficient used are $\epsilon = 1$ and $\nu_1 = 7 \times 10^{-4}$, respectively. The inverse energy transfer rate is $\epsilon_0 = \epsilon - 2\nu_1\Psi_4 = 0.823$, which accounts for 82% of the energy injection rate. The enstrophy range scales as $k^{-5.7}$. Hence, an inverse energy cascade carrying 18% of the energy injection rate is realized in the complete absence of a direct cascade. The theoretical predictions are discussed in Section 4.

The steep enstrophy-range spectra in Figs. 1 and 2 seem to suggest that the present resolutions, particularly the higher one with 2048^2 total modes, may be sufficient to resolve higher Reynolds numbers. It turns out, however, that further decrease of ν_1 leads to spurious dynamics. For example, for $\nu_1 = 3.5 \times 10^{-4}$, 2.5×10^{-4} , the $k^{-5/3}$ inverse-cascading range is distorted after the energy peak has reached $k \approx 8$ (at $t \approx 3.5$): the energy range becomes shallower, due to a spectral rise at the forcing region. It is not known whether this phenomenon is due to finite-size or finite-resolution effects or both. (Such a rise is not observable in the previous simulations, where an inverse-cascading range is established down to $k \approx 3$ without any significant departure from the expected $-5/3$ slope.) A reason to suggest that this phenomenon is mainly a manifestation of finite-resolution effects is that in these cases, the palinstrophy quickly grows to exceed its equilibrium value $\Psi_6 = s^2\epsilon/2\nu_1$ with most of the (resolved) enstrophy range shallower than k^{-5} (see Fig. 4, for example), indicating insufficient resolution for the transient dynamics: a significant amount of palinstrophy would be carried by the unresolved (truncated) wavenumbers. The subsequent evolution of the enstrophy range, confined within the insufficient-resolution range, was observed to cause

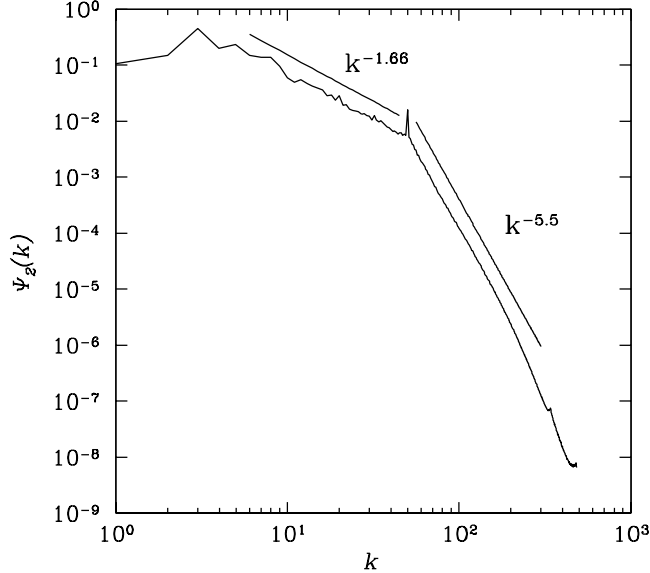


Fig. 2. The energy spectrum $\Psi_2(k)$ vs. k averaged between $t = 8.8$ and $t = 8.9$. The enstrophy averaged in the same period is $\Psi_4 = 761$. The energy injection rate and viscosity coefficient used are $\epsilon = 1$ and $\nu_1 = 5 \times 10^{-4}$, respectively. The inverse energy transfer rate is $\epsilon_0 = \epsilon - 2\nu_1\Psi_4 = 0.761$, which accounts for 76% of the energy injection rate. The enstrophy range scales as $k^{-5.5}$. Hence, an inverse energy cascade carrying 24% of the energy injection rate is realized in the complete absence of a direct cascade. The theoretical predictions are discussed in Section 4.

a rise of the spectrum around s . A growth of enstrophy is induced, thereby interfering with the inverse energy cascade. This phenomenon may be viewed as a redistribution of a significant palinstrophy amount back to the forcing region. This dynamical behaviour is illustrated by Fig. 3, from which the energy range is seen to deviate considerably from the Kolmogorov–Kraichnan $k^{-5/3}$ spectrum.

Higher Reynolds numbers seem to produce shallower enstrophy range during the transient dynamics. For $\nu_1 = 1.25 \times 10^{-4}$ ($\nu_1 = 6.25 \times 10^{-5}$), Fig. 4 (Fig. 5) shows the energy spectrum averaged between $t = 1.1$ ($t = 0.90$) and $t = 1.2$ ($t = 0.95$), during which time about $0.7t_s$ ($0.3t_s$) has elapsed. The transient enstrophy range scales as $k^{-4.5}$ ($k^{-4.1}$) and extends to $k_\nu \approx 500 = 10s$ ($k_\nu > 10s$).⁷ The enstrophy dynamics have become fully dissipative since the palinstrophy has already reached $\Psi_6(1.1) \approx 1.05 \times 10^7$ ($\Psi_6(0.9) \approx 2.15 \times 10^7$), slightly exceeding its equilibrium value $s^2\epsilon/2\nu_1 = 1 \times 10^7$ ($s^2\epsilon/2\nu_1 = 2 \times 10^7$). Clearly, the present resolution is insufficient, and the subsequent evolution is

⁷ Since the formation of an enstrophy range steeper than (but possibly arbitrarily close to) k^{-3} requires virtually no enstrophy to be transferred to its higher-wavenumber end, the enstrophy range may acquire a slope between -5 and -3 during the transient stage. The width and slope of this range should depend on the Reynolds number and evolve with time.

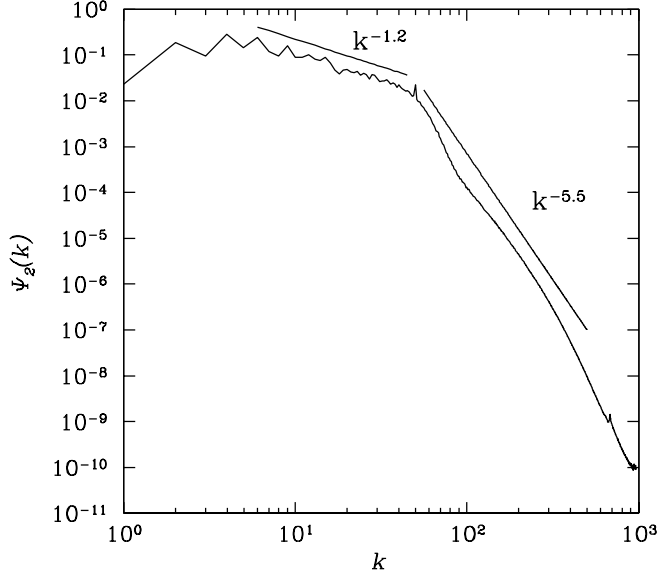


Fig. 3. The energy spectrum $\Psi_2(k)$ vs. k averaged between $t = 7.74$ and $t = 7.84$. The enstrophy injection rate and viscosity coefficient used are $s^2\epsilon \approx 2500$ and $\nu_1 = 2.5 \times 10^{-4}$, respectively. The energy range is significantly shallower than $k^{-5/3}$, due to a rise of the spectrum around s . This rise occurs (and persists) as the palinstrophy evolves within the insufficient-resolution range, after exceeding its equilibrium value $\approx 5 \times 10^6$ (achieving the value 5.26×10^6 at $t \approx 1.2$) with an enstrophy-range slope ≈ -5 .

supposed to suffer from what have been termed “finite-resolution effects” as is seen in the case $\nu_1 = 2.5 \times 10^{-4}$. Apparently, the non-direct-cascading picture would not apply to this stage, nor would it apply to the subsequent dynamics if a persistent direct cascade could be established, withstanding any significant adjustments of the enstrophy-range spectrum. Rather, the realization of this picture requires that the enstrophy range relax toward a k^{-5} spectrum. This relaxation would essentially involve a redistribution of palinstrophy (which has already achieved its equilibrium value $\Psi_6 \approx s^2\epsilon/2\nu_1$) in the wavenumber range $k > s$. In some sense, the realizability of the non-direct-cascading picture requires that any direct-cascading states, regardless of the enstrophy-range slope, be “unstable” and that the palinstrophy be “free” to redistribute itself, until a k^{-5} spectrum can be achieved. This dynamical description is supposed to be what subsequently occurs to the transient states depicted by Figs. 4 and 5 (provided sufficient resolutions). In any case, the realization of transient direct-cascading dynamics, for $\nu_1 = 2.5 \times 10^{-4}; 6.25 \times 10^{-5}$, suggests that for high Reynolds numbers, a transient direct-cascading stage would precede the non-direct-cascading picture if such a picture could be realizable.

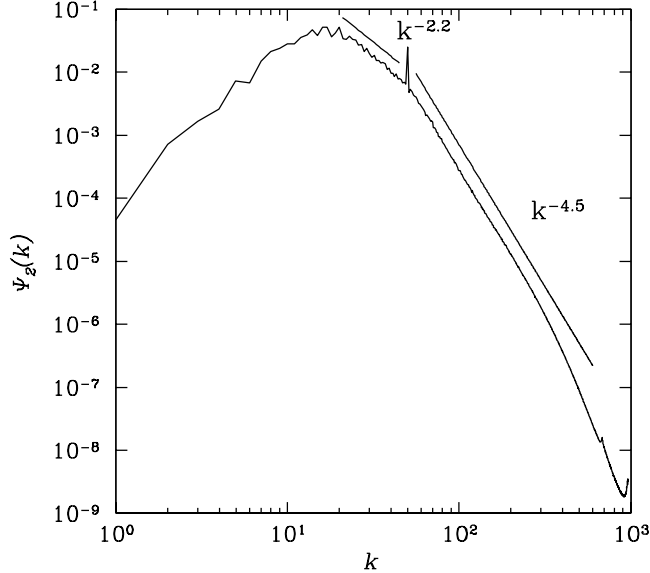


Fig. 4. The energy spectrum $\Psi_2(k)$ vs. k averaged between $t = 1.1$ and $t = 1.2$. The palinstrophy Ψ_6 averaged in the same period is 1.05×10^7 . The respective enstrophy injection rate and viscosity coefficient used are $s^2\epsilon \approx 2500$ and $\nu_1 = 1.25 \times 10^{-4}$, which amount to the palinstrophy equilibrium value $\approx 1 \times 10^7$. One observes that the palinstrophy exceeds its equilibrium value well before a $k^{-5/3}$ spectrum is formed in the energy range. The enstrophy range is shallower than k^{-5} , clearly indicating insufficient resolution for the subsequent evolution.

8 Concluding remarks

The nonlinear transfer and asymptotic dynamical behaviours of α turbulence have been investigated in this work. The results obtained include several estimates on the dynamical quantities, such as the dissipation of the inverse-cascading candidate, and various constraints on the spectral distribution of energy. The conservative transfer of quadratic invariants and the non-conservative transfer of other quadratic quantities are investigated. The possibility of a direct cascade in unbounded fluids is examined by exploring the constraint imposed by the conservative transfer of the advective term. A condition for the possible onset of direct cascade is derived, from which the dual-cascade hypothesis is reformulated. The realization of an inverse energy cascade in the complete absence of a direct enstrophy cascade in 2D NS turbulence is confirmed by numerical simulations.

For systems driven by a forcing spectrally localized at wavenumber s (in the sense discussed in Section 3) and dissipated by a viscous operator $\nu_\mu(-\Delta)^\mu$, where $\nu_\mu > 0$ and $\mu \geq 0$, the invariants $\Psi_{2\alpha}$ and Ψ_α satisfy $\Psi_{2\alpha} \leq s^\alpha \Psi_\alpha$. The nonlinear transfer destroys (creates) the quadratic quantity Ψ_θ for $\theta \in (\alpha, 2\alpha)$ ($\theta \notin [\alpha, 2\alpha]$). This phenomenon allows for vorticity to be created for systems with $\alpha < 2$, which include the SQG equation. The enstrophy

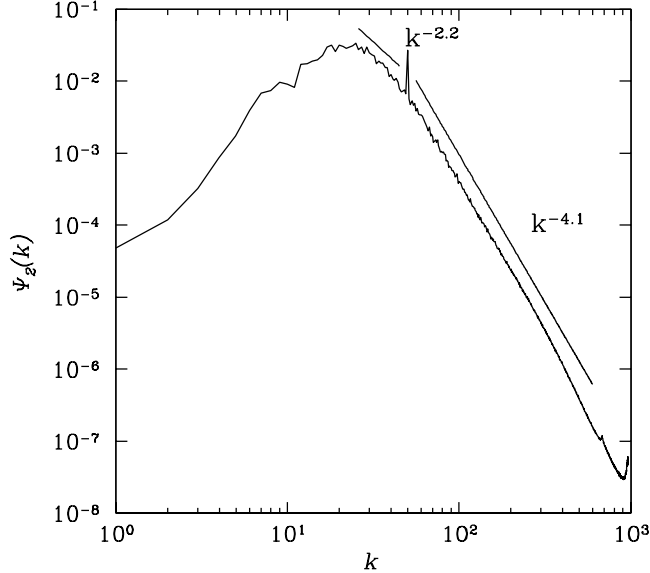


Fig. 5. The energy spectrum $\Psi_2(k)$ vs. k averaged between $t = 0.90$ and $t = 0.95$. The palinstrophy Ψ_6 averaged in the same period is 2.15×10^7 . The respective enstrophy injection rate and viscosity coefficient used are $s^2\epsilon \approx 2500$ and $\nu_1 = 6.25 \times 10^{-5}$, which amount to the palinstrophy equilibrium value $\approx 2 \times 10^7$. One observes that the palinstrophy exceeds its equilibrium value well before a $k^{-5/3}$ spectrum is formed in the energy range. The enstrophy range is shallower than k^{-5} , clearly indicating insufficient resolution for the subsequent evolution.

creation occurs in the high wavenumbers, and the created enstrophy is subject to viscous dissipation. For systems with $\alpha > 2$, such as the RSF equation, energy is created. The creation of energy in RSF turbulence occurs in the low-wavenumber region. In the presence of a persistent inverse cascade, this energy creation would occur at an ever-growing rate.

Fjørtoft-type arguments, based on the two conservation laws of 2D NS turbulence, are reformulated for α turbulence, in an attempt to gain more insights into the possibility of a direct cascade. It is shown that a weak inverse cascade, one that does not carry virtually all of the injection of Ψ_α to ever-larger scales, cannot co-exist with a direct cascade of $\Psi_{2\alpha}$. In order for a direct cascade to be permitted (not to say that it actually occurs), the inverse cascade is required to proceed toward the vanishing wavenumbers, carrying with it virtually all of the injection of Ψ_α . This strong inverse cascade is widely believed to be what happens in the limit of infinite Reynolds number, according to the classical dual-cascade hypothesis. However, it is argued in this present paper that a dynamical picture that features no direct cascade for all Reynolds numbers is self-consistent and possible. This result considerably narrows down the possibility of a direct cascade and also explains the robustness of the inverse energy cascade observed in numerical simulations of 2D NS turbulence, regardless of what happens to the enstrophy [4,5,12,32]. Furthermore, this hypothetical picture serves as a common dynamical background for both

bounded and unbounded fluids. In both cases, no direct cascade would occur for all Reynolds numbers, and differences would arise only when the inverse cascade gets reflected by the largest available scale in the bounded case.

For α turbulence confined to a periodic domain, with a viscous dissipation operator $(-\Delta)^\mu$ ($\mu \geq 0$) the only dissipation mechanism, no direct cascade is permitted. Moreover, an inverse cascade is not possible if the range of wavenumbers lower than the forcing wavenumber is sufficiently wide. More precisely, if the forcing wavenumber s is no smaller than the geometric mean $\sqrt{k_0 k_\nu}$ of the integral wavenumber k_0 (corresponding to the system size) and the dissipation wavenumber k_ν (the wavenumber beyond which the spectrum becomes steeper), then an inverse cascade is not possible. For $s < \sqrt{k_0 k_\nu}$, an inverse cascade cannot be ruled out; however, such a cascade would only be marginal and characteristically different from the inverse cascade in the classical picture for unbounded systems. These results are the generalized versions of those obtained in [30,33] for the NS system. They also apply to unbounded fluids in equilibrium (if such an equilibrium could be achieved), where k_0 is a wavenumber cutoff.

Numerical analyses on 2D NS turbulence have been performed to confirm that a weak inverse energy cascade is realizable in the complete absence of a direct enstrophy cascade. In particular, it is shown that an inverse energy cascade, carrying approximately 24% (18%) of the energy injection to the large scales, is realized and accompanied by a $k^{-5.5}$ ($k^{-5.7}$) enstrophy range. The results also suggest that the inverse-cascading strength (enstrophy-range spectrum) becomes stronger (shallower) as the Reynolds number increases and that for high Reynolds numbers, the non-direct-cascading picture (if it could be realizable) would be preceded by a transient direct-cascading stage. Unfortunately, due to resolution limitation, the numerics fall short on addressing quantitatively how the non-direct-cascading picture evolves with progressively higher Reynolds numbers. This open problem undoubtedly holds the key to a better understanding of the many aspects of finite-Reynolds number turbulence, possibly including the dual-cascade hypothesis in the limit of infinite Reynolds number. In the most favourable scenario, in which the KLB theory should turn out to be correct, a knowledge of this problem would be an asset for formulating a more complete theory of 2D NS turbulence. In particular, the new theory would have to address the dynamics corresponding to the (huge) spectral “gap” between the critical -5 power-law scaling and the -3 power-law scaling of KLB theory (with or without a logarithmic correction). Intuitively, this “gap” would have to be filled with progressively higher Reynolds numbers, starting from the critical Reynolds number corresponding to the onset of a direct enstrophy cascade.

Acknowledgements

The author would like to thank the two anonymous referees for their constructive comments, which helped him clarify and improve the manuscript. He would also like to thank John Bowman for the numerical codes used in Section 7. This work was supported primarily by a Pacific Institute for the Mathematical Sciences postdoctoral fellowship. It was also supported in part by the Natural Sciences and Engineering Research Council of Canada through John Bowman's discovery grant.

References

- [1] C.N. Baroud, B.B. Plapp, Z.-S. She, H.L. Swinney, Anomalous self-similarity in a turbulent rapidly rotating fluid, *Phys. Rev. Lett.* 88 (2002) 114501.
- [2] G.K. Batchelor, Computation of the energy spectrum in homogeneous two-dimensional turbulence, *Phys. Fluids* 12 (II) (1969) 233–239.
- [3] W. Blumen, Uniform potential vorticity flow, Part I: Theory of wave interactions and two-dimensional turbulence, *J. Atmos. Sci.* 35 (1978) 774–783.
- [4] G. Boffetta, A. Celani, M. Vergassola, Inverse energy cascade in two-dimensional turbulence: Deviations from Gaussian behaviour, *Phys. Rev. E* 61 (2000) R29–R32.
- [5] V. Borue, Inverse energy cascade in stationary two-dimensional homogeneous turbulence, *Phys. Rev. Lett.* 72 (1994) 1475–1478.
- [6] J.G. Charney, On the scale of atmospheric motions, *Geof. Publ.* 17 (1948) 3–17.
- [7] P. Constantin, Geometric statistics in turbulence, *SIAM Rev.* 36 (1994) 73–98.
- [8] P. Constantin, Energy spectrum of quasigeostrophic turbulence, *Phys. Rev. Lett.* 89 (2002) 184501.
- [9] P. Constantin, A.J. Majda, E.G. Tabak, Singular front formation in a model for quasigeostrophic flow, *Phys. Fluids* 6 (1994) 9–11.
- [10] R. Fjørtoft, On the changes in spectral distribution of kinetic energy for twodimensional nondivergent flow, *Tellus* 5 (1953) 225–230.
- [11] U. Frisch, *Turbulence: The Legacy of A. N. Kolmogorov*, Cambridge University Press, Cambridge, 1995.
- [12] U. Frisch, P.L. Sulem, Numerical simulation of the inverse cascade in two-dimensional turbulence, *Phys. Fluids* 27 (1984) 1921–1923.
- [13] A. Hasegawa, K. Mima, Pseudo-three-dimensional turbulence in magnetized nonuniform plasma, *Phys. Fluids* 21 (1978) 87–92.
- [14] A. Hasegawa and C.G. MacLennan and Y. Kodama, Nonlinear behavior and turbulence spectra of drift waves and Rossby waves, *Phys. Fluids* 22 (1979) 2122–2129.

- [15] I.M. Held, R.T. Pierrehumbert, S.T. Garner, K.L. Swanson, Surface quasi-geostrophic dynamics, *J. Fluid Mech.* 282 (1995) 1–20.
- [16] R.H. Kraichnan, Inertial ranges in two-dimensional turbulence, *Phys. Fluids* 10 (1967) 1417–1423.
- [17] R.H. Kraichnan, Inertial-range transfer in two- and three-dimensional turbulence, *J. Fluid Mech.* 47 (1971) 525–535.
- [18] C.E. Leith, Diffusion approximation for two-dimensional turbulence, *Phys. Fluids* 11 (1968) 671–673.
- [19] M.E. Maltrud, G.K. Vallis, Energy spectra and coherent structures in forced two-dimensional and beta-plane turbulence, *J. Fluid Mech.* 228 (1991) 321–342.
- [20] H.K. Moffatt, *Advances in Turbulence*, Springer–Verlag, Berlin, 1986.
- [21] K. Ohkitani, M. Yamada, Inviscid and inviscid-limit behavior of a surface quasigeostrophic flow, *Phys. Fluid* 9 (1997) 876–882.
- [22] J. Pedlosky, *Geophysical Fluid Dynamics*, 2nd edition, Springer–Verlag, New York, 1987.
- [23] R.T. Pierrehumbert, I.M. Held, K.L. Swanson, Spectra of local and nonlocal two-dimensional turbulence, *Chaos, Solitons and Fractals*, 4 (1994) 1111–1116.
- [24] P.G. Saffman, On the spectrum and decay of random two-dimensional vorticity distribution of large Reynolds number, *Stud. Appl. Math.* 50 (1971) 377–383.
- [25] N. Schorghofer, Universality of probability distributions among two-dimensional turbulence flows, *Phys. Rev. E* 61 (2000) 6568–6571.
- [26] N. Schorghofer, Energy spectra of steady two-dimensional turbulence flows, *Phys. Rev. E* 61 (2000) 6572–6577.
- [27] T.G. Shepherd, Rossby waves and two-dimensional turbulence in a large-scale zonal jet, *J. Fluid Mech.* 183 (1987) 467–509.
- [28] K.S. Smith, G. Boccaletti, C.C. Henning, I. Marinov, C.Y. Tam, I.M. Held, G.K. Vallis, Turbulent diffusion in the geostrophic inverse cascade, *J. Fluid Mech.* 469 (2002) 13–48.
- [29] P.L. Sulem, U. Frisch, Bounds on energy flux for finite energy turbulence, *J. Fluid Mech.* 72 (1975) 417–423.
- [30] C.V. Tran, J.C. Bowman, On the dual cascade in two-dimensional turbulence, *Physica D* 176 (2003) 242–255.
- [31] C.V. Tran, J.C. Bowman, Energy budgets in Charney–Hasegawa–Mima and surface quasigeostrophic turbulence, *Phys. Rev. E* 68 (2003) 036304.
- [32] C.V. Tran, J.C. Bowman, Robustness of the inverse cascade in two-dimensional turbulence, *Phys. Rev. E* 69 (2004), in press.

- [33] C.V. Tran, T.G. Shepherd, Constraints on the spectral distribution of energy and enstrophy dissipation in forced two-dimensional turbulence, *Physica D* 165 (2002) 199–212.
- [34] K.K. Tung, W.W. Orlando, On the differences between 2D and QG turbulence, *Discrete Contin. Dyn. Syst. Ser. B* 3 (2) (2003) 145–162.
- [35] S. Weinstein, P. Olson, D. Yuen, Time-dependent large aspect-ratio thermal-convection in the earths mantle, *Geophys. Astrophys. Fluid Dyn.* 47 (1989) 157–197.